Estimating ocean surface meteorology from passive microwave observations for the development of satellite-derived turbulent fluxes

J. Brent Roberts[1], Clay Blankenship[2], Sayak Biswas[2], Carol Anne Clayson[3],
[1]NASA MSFC, [2]Universities Space Research Association, [3]WHOI

Introduction and Motivation

The surface turbulent fluxes of moisture and heat are essential components of the global energy and water cycles. Estimation of these fluxes across the global oceans requires the knowledge and application of four surface bulk variables to a suitable bulk flux algorithm: i) wind speed (Wspd), ii) air specific humidity (Qair), iii) air temperature (Tair), and surface skin temperature (SST).

Moored buoys and voluntary observing ships (VOS) provide a valuable standard for evaluation, but they are quite sparse resulting in large sampling uncertainties of the bulk variables, especially at monthly and shorter time scales. This leads to increased uncertainties in the large-scale estimates of surface fluxes from *in situ* measurements alone.

Global coverage by VOS is hampered by the requirements of simultaneous measurements of all 4 bulk parameters and associated observing height metadata. There has been a recent, steady decline in VOS observations and their global coverage; a nearly 15% drop in areal coverage is evident since the late 1980's.

Passive microwave observations provide an alternative source for estimating the near-surface bulk variables and hence the surface turbulent fluxes. They provide significantly improved global coverage at daily time scales and thus narrow sampling uncertainties especially for monthly and annual means.

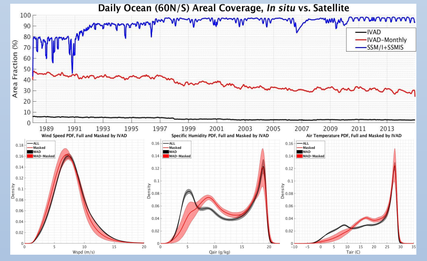

The areal coverage of near-surface bulk variables over the ocean is shown for VOS (IVAD) and passive microwave imagers for a day. A 31-day moving window also illustrates the expected coverage for IVAD when averaging at monthly time periods.

Estimates of the distribution (PDF) are shown for Wspd, Qair, and Tair based on the full and sub-sampled by IVAD ("Masked") SeaFlux Climate Data Record. Shading represents the range of PDF estimates for individual months. Note the larger monthly PDF variability for Masked.

Surface Retrievals

From statistical decision theory, finding a "best" model for predicting a response variable—for squared error loss— results in the optimal solution (Hastie et al. 2009):

$$\boldsymbol{f(x) = E(Y|X = x)}$$ ***, i.e. the conditional expectation***

Different retrieval algorithms diverge with respect to how one approximates this conditional expectation given potential *a priori* constraints and sources of information.

Passive microwave imagers and sounders have been designed to observe at frequencies that provide information SST, Wspd, Qair, and to a lesser extent Tair.

While microwaves do transmit through clouds, cloud liquid (and rain) water emission remains a major component of the observed signal and obscures the surface signal.

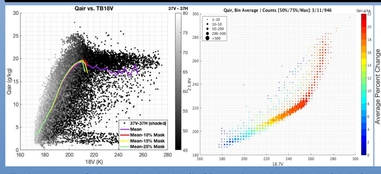

Estimates of the univariate (left) and multivariate (right) conditional mean for Qair is shown for a large collocation dataset of microwave imager and buoy observations. For the univariate case, note the impact on the conditional mean as cloud liquid water is masked.

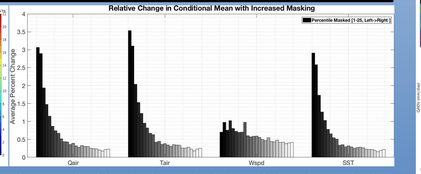

As more liquid water is masked, the relative change in the conditional mean decreases rapidly due the nonlinear impacts of liquid water emission. After masking 10% of observations, the relative changes fall below ~0.5% per 1% increase of the mask for all 4 surface variables.

Validation of Surface Parameters

A neural network has been trained to estimate the surface bulk variables using data from SSMIS, AMSR-2, and GMI collocated with quality-controlled moored surface buoys.

The relationships are robust and reproducible between sensors and for varying differences in the underlying collocation datasets and levels of cloud/rain masking.

Overall, these retrievals exhibit small total biases, root-mean-square errors on par with reanalyses, and significant correlation. However, conditional biases do remain particularly towards the extremes (both low and high) of the distributions.

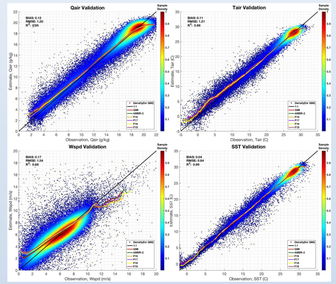

Density (shaded) scatterplots of the observed and estimated parameters using a validation dataset are shown for each surface parameter. Binned means are shown for each sensor and the 1:1 line for reference. Note the consistency between the individual sensors.

Regional Biases and Dynamical Regimes

Several independent efforts are being made to estimate satellite-derived surface turbulent heat fluxes. These generally use similar sets of channels from passive microwave instruments but diverge with respect to the use of first-guess information, statistical regression technique, and surface training datasets.

Studies have observed large-scale regional patterns of biases in several of these products thus bringing into question the independence of errors. Investigation of these patterns reveals they are geographically co-aligned with known large-scale dynamical regimes and cloud structures.

Wong et al. (2016) decomposed the integrated water budget tendency equation as:

$$P - E + \frac{\partial Q}{\partial t} = -Q\nabla \cdot \boldsymbol{V} - \boldsymbol{V} \cdot \nabla Q = QCON + QADV$$

where Q represents vertically integrated water vapor and $\boldsymbol{V}$ is the scaled vertically integrated ***vector*** moisture flux.

Analyses revealed large-scale patterns of ascent/descent and convective instability with respect to dynamical convergence and moisture advection. Here, we show that large-scale cloud regimes as identified by ISCCP Global Weather States also share significant overlap with regimes as defined in this moist-dynamics phase space. Further, the large-scale conditional biases observed in several of the latest-generation satellite derived products are distinctly stratified as well.

We can relate the large-scales controls on the dynamics to the generation of clouds (which impact the retrievals) alteration of the vertical distribution of water vapor within these regimes. Both features result in conditional errors in the surface retrievals, particularly for surface humidity as imagers provide very limited vertically-resolved information.

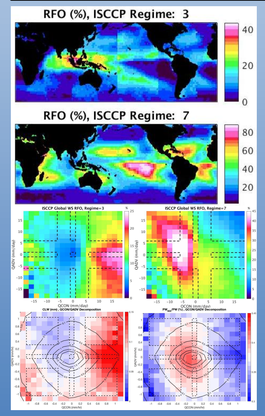

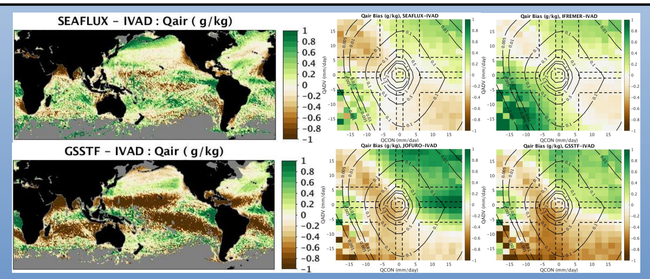

(Left) The relative frequency of occurrence (RFO) is shown for two ISCCP regimes — 3 and 7 — representing respectively stratiform anvils with mid-level congestus and fair-weather cumulus. The RFO is also shown within the QCON-QADV phase-diagram; note the significant concentration of each regime in different quadrants of this space. Also shown are the fields of MERRA-2 cloud liquid water and the ratio of Surface-900mb water vapor to Q.
(Above) Maps of annual mean biases are shown for two passive microwave estimates of Qair validated with VOS observations. Biases are also shown as stratified within the QCON-QADV phase space for both these and an additional two products that exhibit similar geographic structures. Note the strong partitioning of biases in this space.

State-Dependent Bias Corrections

The systematic error of an estimate, y, can be represented at the total, weighted contribution of bias errors, δ, from a set of K individual regimes as:

$$Bias = E(y - x) = \sum_{k=1}^{K} w_k \delta_k$$

where the weight is the relative frequency of occurrence of that regime. Rather than implementing a constant bias correction at a location, we can thus develop a bias correction that is applied with respect to individual regimes.

Here, we consider each bin in the QCON-QADV phase diagram as a regime and apply a state-dependent bias correction to different satellite-derived Qair estimates. Because the regimes exhibit strong concentration in space (as controlled by large-scale dynamics) so to do the time-mean bias correction patterns.

On a daily timescale, however, the bias correction show substantial variability and are organized by the prevailing dynamical state during that day.

The bias correction can not fully eliminate the biases, however, as the bias is conditioned across all locations. Nevertheless, substantial mitigation of biases — as tuned for each product — is achievable resulting in more consistent and accurate satellite-derived Qair estimates.

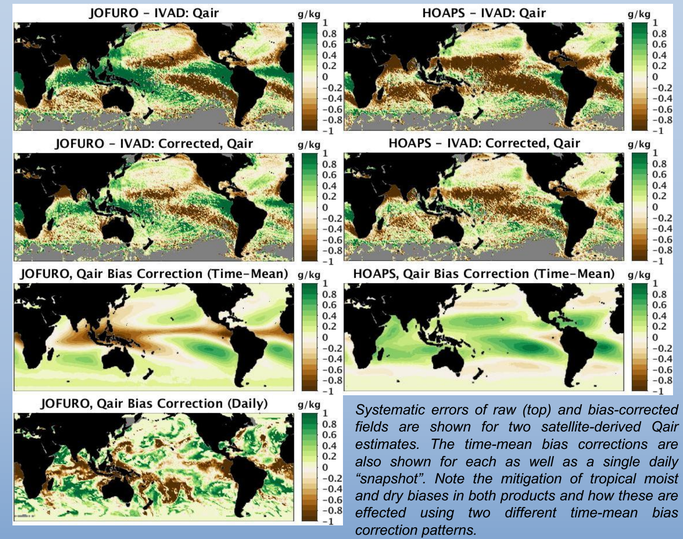

Systematic errors of raw (top) and bias-corrected fields are shown for two satellite-derived Qair estimates. The time-mean bias corrections are also shown for each as well as a single daily "snapshot". Note the mitigation of tropical moist and dry biases in both products and how these are effected using two different time-mean bias correction patterns.

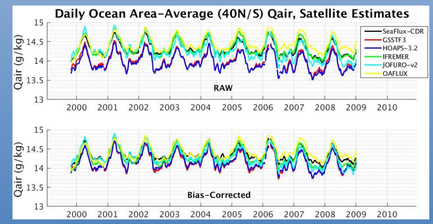

Area-average time series of Qair are shown for 6 different satellite-derived estimates for both raw (top) and bias-corrected fields over the common observing period 1999-2008. Note how the state-dependent bias correction results in more consistent — and presumably more accurate with reference to VOS — surface estimates across the products.